Received: 4 July 2021 | Revised: 18 October 2021 | Accepted: 25 October 2021

DOI: 10.1111/joa.13584

Journal of Anatomy | ANATOMICAL SOCIETY WILEY

REVIEW ARTICLE

Typical *m. triceps surae* morphology and architecture measurement from 0 to 18 years: A narrative review

Matthew Bell[1] | Ghaliya Al Masruri[1] | Justin Fernandez[2,3] | Sîan A. Williams[4,5] | Anne M. Agur[6] | Ngaire S. Stott[5] | Behzad Hajarizadeh[7] | Ali Mirjalili[1]

[1]Department of Anatomy and Medical Imaging, Faculty of Medical and Health Sciences, University of Auckland, Auckland, New Zealand

[2]Auckland Bioengineering Institute, University of Auckland, Auckland, New Zealand

[3]Department of Engineering Science, University of Auckland, Auckland, New Zealand

[4]Faculty of Health Sciences, Curtin School of Allied Health, Curtin University, Perth, Australia

[5]Faculty of Medical and Health Sciences, Department of Surgery, University of Auckland, Auckland, New Zealand

[6]Division of Anatomy, Department of Surgery, Faculty of Medicine, University of Toronto, Toronto, Canada

[7]The Kirby Institute, UNSW Sydney, Sydney, Australia

Correspondence
Ali Mirjalili, Faculty of Medical and Health Sciences, Department of Anatomy and Medical Imaging, University of Auckland, Auckland, New Zealand.
Email: a.mirjalili@auckland.ac.nz

Abstract

The aim of this review was to report on the imaging modalities used to assess morphological and architectural properties of the *m. triceps surae* muscle in typically developing children, and the available reliability analyses. Scopus and MEDLINE (Pubmed) were searched systematically for all original articles published up to September 2020 measuring morphological and architectural properties of the *m. triceps surae* in typically developing children (18 years or under). Thirty eligible studies were included in this analysis, measuring fibre bundle length (FBL) (n = 11), pennation angle (PA) (n = 10), muscle volume (MV) (n = 16) and physiological cross-sectional area (PCSA) (n = 4). Three primary imaging modalities were utilised to assess these architectural parameters *in vivo*: two-dimensional ultrasound (2DUS; n = 12), three-dimensional ultrasound (3DUS; n = 9) and magnetic resonance imaging (MRI; n = 6). The mean age of participants ranged from 1.4 years to 18 years old. There was an apparent increase in *m. gastrocnemius medialis* MV and pCSA with age; however, no trend was evident with FBL or PA. Analysis of correlations of muscle variables with age was limited by a lack of longitudinal data and methodological variations between studies affecting outcomes. Only five studies evaluated the reliability of the methods. Imaging methodologies such as MRI and US may provide valuable insight into the development of skeletal muscle from childhood to adulthood; however, variations in methodological approaches can significantly influence outcomes. Researchers wishing to develop a model of typical muscle development should carry out longitudinal architectural assessment of all muscles comprising the *m. triceps surae* utilising a consistent approach that minimises confounding errors.

KEYWORDS
architectural properties, imaging modalities, musculoskeletal development, paediatrics, triceps surae

1 | INTRODUCTION

Skeletal muscle architecture is a major determinant of muscle function and physical performance (Lieber & Ward, 2011). Architecture refers to the internal configuration of the contractile and connective tissue elements of a muscle. Thus, two muscles with similar external appearances can function differently because of variations in internal structure. Internal muscle architecture can be measured and quantified *in vivo*, with various parameters defining aspects of morphology. These parameters include fibre bundle length (FBL), pennation angle (PA), muscle volume (MV), and physiological cross-sectional area (pCSA).

FBL is defined as the distance from the origin of the most proximal muscle fibres to the insertion of the most distal fibres and determines the excursion capacity of the muscle (Lieber & Fridén, 2000). The greater the FBL, the more sarcomeres in series, and the higher the excursion capacity of the muscle. Hence, a higher FBL allows a greater range through which muscles can generate force and greater maximum shortening velocity (Gans & Vree, 1987). PA is the angle between the direction of muscle fibres and the line of action of the muscle and changes with joint position (Figure 1) (Lee et al., 2015; Lieber & Fridén, 2000). As the PA increases, the component of force along the line of action decreases. However, pennation also allows many more muscle fibres to fit within the same muscle volume, increasing force generation (Lieber, 2011). Additionally, a higher PA is associated with a shorter FBL, reducing velocity. Overall, this indicates that muscles with low PAs are ideal for strong contractions over a short length. MV is an indicator of overall muscle size and is defined as the amount of space taken up by a muscle's connective and contractile tissue (Chelly & Denis, 2001; O'Brien et al., 2009). MV is an important determinant of force generation and physical function. The pCSA is defined as the sum of the cross-sectional areas of all the muscle fibres within the muscle. There is a direct relationship between pCSA and the relative maximum tetanic force produced by a muscle, which can be used to compare the force-producing capabilities of muscles (Lieber & Fridén, 2000; Ravichandiran et al., 2010). The pCSA can be estimated using the following equation with MV, PA and FBL:

$$\text{pCSA} = \text{muscle volume} \times \cos(\text{PA})/\text{FBL}$$

Several different imaging modalities can be used to quantify the architectural parameters of a muscle. The most common modalities are two-dimensional ultrasound (2DUS), three-dimensional ultrasound (3DUS), and magnetic resonance imaging (MRI). Two-dimensional B-mode ultrasound represents a non-invasive, safe and accessible method to assess muscle morphology (Lieber & Ward, 2011; Narici, 1999). It is primarily used in research to quantify FBL and PA (Chen et al., 2018; Kawano et al., 2018; Kruse et al., 2018; Legerlotz et al., 2010; Mathewson et al., 2015; Mohagheghi et al., 2008; Morse et al., 2008; Shortland et al., 2002; Stephensen et al., 2012; Wren et al., 2010). Additionally, 2DUS ultrasound has been used to measure anatomical cross-sectional area (aCSA) and estimate MV (Morse et al., 2015; Park et al., 2014; Schless et al., 2018; Tomlinson et al., 2014; Vanmechelen et al., 2018). 3D ultrasound combines simultaneous 2D B-mode ultrasound imaging with a motion tracking system to track the position and orientation of the probe while scanning (Barber et al., 2009). This allows 3D reconstructions of skeletal muscles to be made from data that can be acquired quickly and non-invasively. MRI represents the gold standard for *in vivo* muscle morphology due to its ability to acquire high-resolution 3D images. 3D ultrasound and MRI have both been used mainly for MV assessment (Barber et al., 2011a, 2011b, 2016; Cenni et al., 2018a; Herskind et al., 2016; Malaiya et al., 2007; Morse et al., 2008; Oberhofer et al., 2010; Obst et al., 2017; Pitcher et al., 2018; Schless et al., 2019a, 2019b; Vanmechelen et al., 2018; Willerslev-Olsen et al., 2018). Using diffusion tensor imaging (DTI) sequencing, it is possible to view muscle fibre bundles and aponeuroses volumetrically to quantify FBL, PA and pCSA.

The *m. gastrocnemius medialis* (MG), *lateralis* (LG) and *m. soleus* (SOL) muscles are skeletal muscles in the posterior compartment of the leg, together comprising the *m. triceps surae* (Moore et al., 2014). The *m. triceps surae* generates 80% of the force required to plantarflex the ankle (Murray et al., 1976), making it essential for locomotion and forward propulsion (Neptune et al., 2001; Standring, 2016). The architecture of the *m. triceps surae* muscle has been described in older children and adults with regards to the structure–function relationship of skeletal muscle. Understanding the normal changes that occur in typically developing individuals (those without pathologies and born on time) is important for

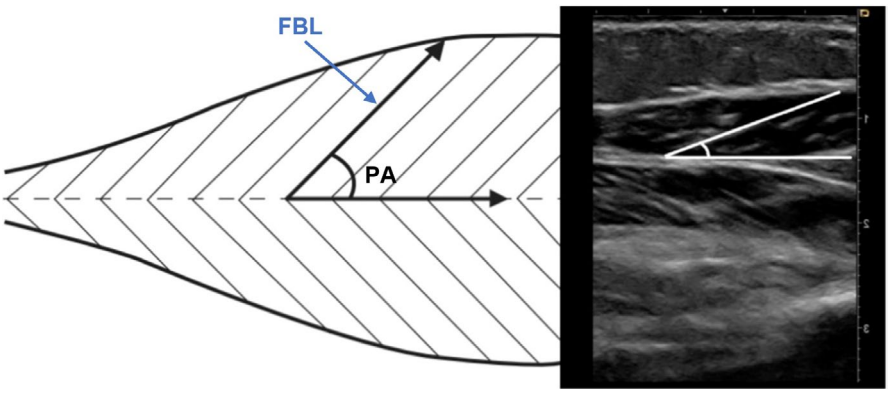

FIGURE 1 FBL and PA schematic illustration (left) ultrasonographic image (right)

comparison with individuals with musculoskeletal disorders such as cerebral palsy (Barber et al., 2011a; Willerslev-Olsen et al., 2018). Increased knowledge of the typical development of the *m. triceps surae* may provide explanations for the functional evolution that occurs during development and growth and facilitate evaluation of the efficacy of interventions.

The primary aim of this review was to investigate the methodologies that have been used to quantify the muscle architecture of the *m. triceps surae* in populations from 0 to 18-years-old, as well as their reliability and limitations. The secondary aim was to analyse the reported muscle architecture of the *m. triceps surae* in populations from 0 to 18-years-old to establish evident age-dependent correlations.

2 | METHODS

A literature search was conducted to find studies that investigated *in vivo* muscle architecture of the *m. triceps surae* (including FBL, PA, MV and PCSA) in participants from 0 to 18 years old. The following terms were searched in titles, abstracts and study keywords for the literature search: ("gastrocnemius" or "soleus") and ("muscle volume" or "pennation angle" or "physiological cross-sectional area" or "fibre bundle length" or "muscle fascicle length"). The search was conducted in two major bibliographic databases, Scopus and MEDLINE (Pubmed), looking for all articles published up until September 2020. Studies were limited to original research, published in English, with short communications and conference proceedings excluded. Articles were included within the review if they investigated the muscles of the *m. triceps surae* of healthy, typically developing children (age between 0 and 18 years), with measurements of one or more of the four architectural parameters of interest (FBL, PA, MV and pCSA). Articles were excluded if they did not meet the aforementioned inclusion criteria. Articles were excluded from this review based on an absence of typically developing, human participants (or those with no pathology), participants with a mean age older than 18 years, or an absence of any gross muscle morphological and architectural properties being examined (from FBL, PA, MV and PCSA). Additionally, articles were excluded if they met any of the following conditions not written in English, not a full journal paper. No supplementary data were sought from authors.

2.1 | Data extraction and statistical analysis

Data items were extracted from eligible studies by MB and included: number of participants, mean and standard deviation of participants' age, imaging methods, investigated muscle(s), ankle position and the study outcomes, including mean and standard deviation of FBL, PA, MV and pCSA. Data of each study outcome were presented in separate forest plots. We did not conduct any meta-analysis to cumulate the results, given the heterogeneity of participants' age across studies. The association between participants' mean age and each study outcome was assessed using meta-regression.

3 | RESULTS

As a result of the search, 1379 papers were found. After the exclusion of ineligible studies, 30 papers met all the criteria and were included in the analysis (Figure 2).

The outcomes of this literature review are divided into three parts: imaging techniques, architectural parameters and reliability. First, studies have made use of three primary imaging modalities to investigate muscle architecture in children: 2DUS, 3DUS and MRI. These techniques possess their own strengths and limitations in assessing different parameters. Methodological variations also exist between studies using the same modality, which may affect the interpretation of results and hence represents an important consideration when comparing studies. Secondly, the four architectural parameters that have been included are FBL, PA, MV and pCSA. Finally, reliability assessments of each modality have been investigated from that reported in the included studies. Reliability is an essential measurement in imaging research to ensure that results accurately reflect the true internal 3D muscle architecture. Given the potential utility of *in vivo* imaging techniques in quantifying architectural measurements in longitudinal studies and aid in diagnosis and management in routine clinical practice, ensuring consistent, accurate results is crucial (Brink & Louw, 2012).

3.1 | Imaging techniques

3.1.1 | Two-dimensional ultrasound (2DUS)

Two-dimensional, B-mode (brightness mode) ultrasound was used by 12 studies to measure architectural parameters of the *m. triceps surae* in both children and young adults (Barber et al., 2017; Cenni et al., 2018b; Chen et al., 2018; Kawano et al., 2018; Kruse et al., 2018; Legerlotz et al., 2010; Mathewson et al., 2015; Mohagheghi et al., 2008; Morse et al., 2008; Shortland et al., 2002; Stephensen et al., 2012; Wren et al., 2010). One factor that affects the appearance of tissues is the echogenicity, or the degree to which a tissue reflects or transmits ultrasound waves. Cross-sectional images of tissue generated with this technique display dense connective tissue (such as the epimysium, perimysium or aponeurosis) as appearing hyperechoic, or light grey on the image. This contrasts with the high-water content of muscle fibres causing them to appear hypoechoic, or black on the image.

When B-mode scans are aligned with the muscle fascicles, a striating pattern of muscle fascicles can be visualised (Lichtwark, 2017), allowing measurement of muscle architectural parameters (Bénard et al., 2009). Within the identified studies, the mean age of participants varied from 4.8 to 12.4 years old. Most studies utilising 2DUS have measured FBL and PA (Barber et al., 2017; Cenni et al., 2018b;

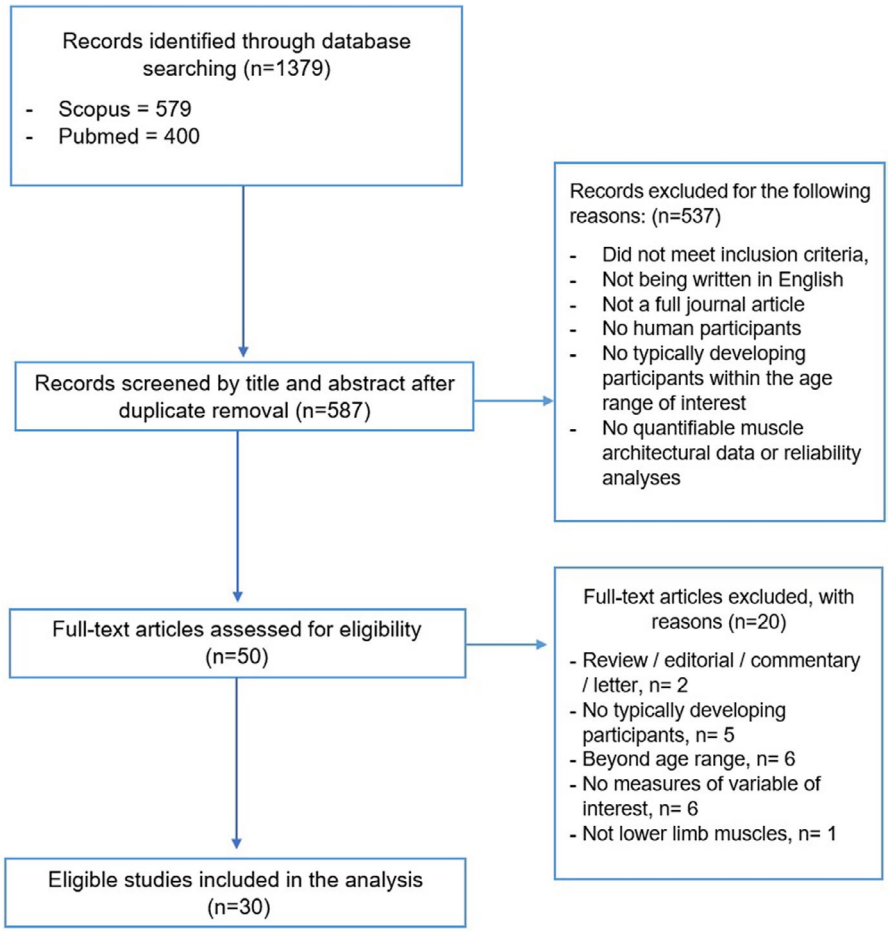

FIGURE 2 Flow diagram of the literature search with study identification, screening and assessment of eligibility for inclusion in this review

Chen et al., 2018; D'Souza et al., 2019; Kawano et al., 2018; Kruse et al., 2018; Legerlotz et al., 2010; Malaiya et al., 2007; Mathewson et al., 2015; Mohagheghi et al., 2008; Morse et al., 2008; Shortland et al., 2002; Stephensen et al., 2012; Wren et al., 2010). Many methodological variations are present between studies utilising 2DUS, including differences in joint position, acquisition technique and ultrasound systems. Table 1 outlines the joint positioning (knee and ankle angle) and location from which FBL/PA were measured. A wide range of transducers and ultrasound systems have been used across the various studies identified in this review (Table 2).

3.1.2 | Three-dimensional ultrasound (3DUS)

3D ultrasonography is an alternative method for measuring *in vivo* muscle architecture and was used in 9 papers (Barber et al., 2011a, 2011b, 2016; Malaiya et al., 2007; Obst et al., 2017; Schless et al., 2018, 2019a, 2019b; Willerslev-Olsen et al., 2018). It combines 2D B-mode ultrasound images and 3D motion analysis to provide a direct in vivo reconstruction of muscle morphology (Figure 3) (Hsu et al., 2009). A stack of 2D images is simultaneously generated while the position and orientation of the ultrasound probe are tracked using 3D motion analysis (Barber et al., 2009; Prager et al., 1998). Determination of MV is achieved with 3D ultrasound by sweeping the ultrasound transducer over the length of the muscle of interest. The muscle boundaries must be included in the stack of images to generate an accurate reconstruction of the muscle shape, allowing for measurement of MV (Figure 3).

Three-dimensional ultrasound (3DUS) is favourable due to its lower cost, portability, safety, high-resolution images and shorter scanning times compared with MRI (Weide et al., 2017). However, 3DUS can require lengthy post-processing time, a motion capture system and trained operators. 3D freehand ultrasound techniques have been validated against MRI for the purposes of MV evaluation *in vivo* (Barber et al., 2009, 2019; Noorkoiv et al., 2019). Studies utilising 3DUS have used a variety of transducers. All used a Telemed Echoblaster 128 system with either a 9 MHz (Barber et al., 2016; Obst et al., 2017) or 10 MHz (Barber et al., 2011a; Cenni et al., 2018b; Schless et al., 2018, 2019a, 2019b; Willerslev-Olsen et al., 2018) linear transducer, but one study used a lower frequency transducer (7.5 MHz) (Malaiya et al., 2007). In addition, three different motion capture systems have been used: Optitrack (Barber et al., 2016; Obst et al., 2017; Schless et al., 2018, 2019a), Vicon (Barber et al., 2011a; Cenni et al., 2018b; Schless et al., 2019b; Willerslev-Olsen et al., 2018) and Compact scan (Malaiya et al., 2007).

TABLE 1 2DUS papers that described joint positioning (knee and ankle angle) and location from which PA/FBL length measurements were made

	Ankle angle	Knee angle	Location along muscle	Contracted/relaxed
Chen et al. (2018)	Held fixed (20° plantarflexion)	Fully extended	Vertical to the surface of the largest circumference of the calf	Each participant lay prone on the examination couch with the distal portion of their legs off the plinth. The ankle angle was fixed by an assistant
Kawano et al. (2018)	Passive maximum dorsiflexion (39.3°)	Extended	Not specified	Participants in resting position with their legs hanging down and in the passive maximum dorsiflexion position of the ankle
Shortland et al. (2002)	Angles: 0°, −15°, −30° and resting (−23.8)	Knee extended	Distal portion of the MG	Each participant lay prone with the distal portion of their legs off the plinth. An assistant maintained the required ankle position during image collection
Mohagheghi et al. (2008)	Resting joint angle 25°	Not stated	Middle region of the MG and LG, at the proximal, middle and distal sections of each muscle head	Participants lay prone on an examination plinth with their feet hanging from its edge during scanning
Malaiya et al. (2007)	Resting And maximum passive dorsiflexion	Knees extended	At a point half way along the length of the muscle and at about half the width of the muscle	Subjects prone, relaxed position of the foot with no external forces applied
Barber et al. (2017)	Measurements taken during gait	Knee extended	Medio-lateral centre of the medial gastrocnemius	Not stated
Cenni et al. (2018b)	Maximum plantarflexion, maximum dorsiflexion, 50% ROM	Knee flexed to 20°	Placed longitudinally over the fascicle plane at the mid-muscle length, along a line drawn between medial femoral condyle and MG MTJ	Participants lay prone on a bed, with the lower leg supported on an inclined cushion. The leg was positioned in a custom-made orthotic to control ankle movement in the sagittal plane
D'Souza et al. (2019)	Mean (123°)	Not stated	The median fascicle lengths and pennation angles of all fascicles in a muscle	Passive conditions
Kruse et al. (2018)	Resting joint angle (−20.8°)	Knees full extended	Not stated	Relaxed position of the foot, with no external force applied. Rest
Wren et al. (2010)	Maximum dorsiflexion (10.9°), Maximum plantarflexion (−35.6°), resting ankle angle (−18.0°)	Not stated	Transducer aligned along the middle of the medial gastrocnemius just proximal to the distal toe of the muscle	Participants lay prone, a dynamometer was used to passively dorsiflex and plantarflex the ankle through the range of motion

3.1.3 | Magnetic resonance imaging

Magnetic Resonance Imaging (MRI) has been used for the assessment of MV and 3D shape reconstruction. Validation for MRI has been carried out against cadaveric muscles (Mitsiopoulos et al., 1998). An advantage of MRI over other imaging modalities is better soft tissue contrast between fat, connective tissue and muscle (Finanger et al., 2012). MRI provides clear superficial and deep images with the same efficacy. Importantly, MRI does not depend on the experience of the operator, unlike 2D and 3D US. However, MRI is expensive, and participants must stay still during image acquisition, which is difficult to achieve in the younger child and infant population and may make this modality impractical for longitudinal studies.

Diffusion Tensor Imaging (DTI) is an MRI technique and is one of the most recently developed methods of imaging musculoskeletal architecture. DTI-based measurements of architecture rely on the principle that the diffusion rate of water molecules is higher in the longitudinal direction of the muscle fibres than in the fibres transverse plane. It can be used to generate high resolution, 3D reconstructions of muscle architecture *in vivo*. DTI measures, for each voxel, the direction in which diffusion rates are the highest, providing a local measure of muscle fibre orientation. 3D reconstructions generate curves (called fibre tracts) that propagate along the primary diffusion direction throughout the muscle. Fibre tracts follow the direction of muscle fibres and can thus be used to obtain quantitative measures of 3D muscle architecture such as FBL and PA, unlike other MRI sequences. While the use of DTI to examine skeletal muscle architecture has become increasingly common, only one study has utilised DTI within a child population (D'Souza et al., 2019) and no aponeuroses were visualised (Bolsterlee et al., 2018).

TABLE 2 The methodology of 2DUS studies

Study	Ultrasound system and transducer (field of view where available)
Chen et al. (2018)	Siemens Acuson 5000 and a 11 MHz linear ultrasound probe (50 mm field of view)
Kawano et al. (2018)	Logiq 7, GE Healthcare and a 9 MHz linear ultrasound probe (50 mm field of view)
Legerlotz et al. (2010)	Phillips HD11 Real-Time Ultrasound Machine and a 7.5 MHz linear ultrasound probe
Shortland et al. (2002)	Esaote Biomedica and a 7.5 or 10 MHz linear ultrasound probe
Cenni et al. (2018b)	Telemed Echoblaster 128 and a 10 MHz linear ultrasound probe (59 mm field of view)
Barber et al. (2017)	Telemed Echoblaster 128 and a 5 MHz linear ultrasound probe (60 mm field of view)
Wren et al. (2010)	Portable Terason ultrasound system and a 5–10 MHz linear ultrasound probe
Mohagheghi et al. (2008)	ALOKA SSD-5000 and 10 MHz linear ultrasound probe or Esaote SpA and a 12 MHz linear ultrasound probe
Stephensen et al. (2012)	Diasus Application Specific Ultrasound System and a 5–10 MHz linear array transducer (65 mm field of view)
Morse et al. (2008)	HDI-3000, ATL and a 7.5 MHz linear ultrasound probe
Kruse et al. (2018)	LA 923, Esaote and a 10 MHz linear ultrasound probe (100 mm field of view)
Mathewson et al. (2015)	t3200 Terason portable ultrasound system and a 4–15 MHz linear ultrasound probe

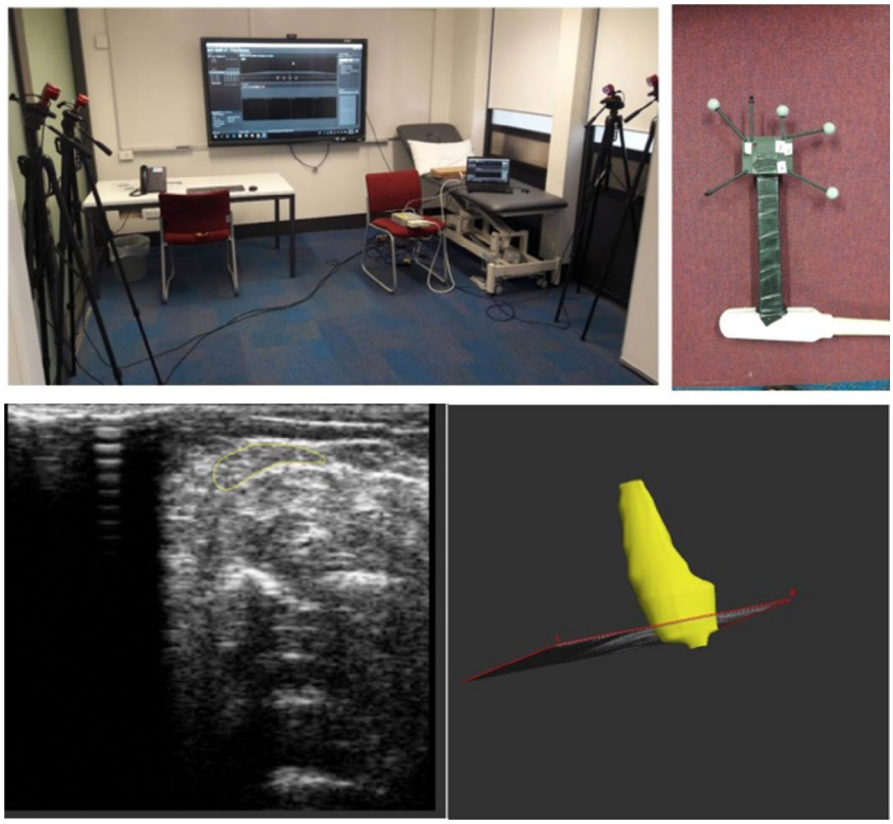

FIGURE 3 3D ultrasound motion analysis set up (top left) Ultrasound transducer with attached reflective markers (top right). An image segmentation (bottom left). 3D reconstruction of a medial gastrocnemius using Stradwin software (bottom right)

We identified six studies that reported on MRI acquired muscle morphology in our target cohort (D'Souza et al., 2019; Herskind et al., 2016; Morse et al., 2008; Oberhofer et al., 2010; Pitcher et al., 2018; Vanmechelen et al., 2018). Methodological variations existed between studies in the scanner and sequence that was used. Several opted for either a 3T scanner (D'Souza et al., 2019; Herskind et al., 2016; Vanmechelen et al., 2018), or a 1.5T scanner (Oberhofer et al., 2010; Pitcher et al., 2018; Vanmechelen et al., 2018) and one a 0.2T scanner (Morse et al., 2008). Additionally, the T1-weighted sequence is the most commonly used sequence (Morse et al., 2008; Pitcher et al., 2018), with alternative sequences being Three-point Dixon sequence (Vanmechelen et al., 2018) and DTI (D'Souza et al., 2019). Two papers did not describe which sequence was used (Herskind et al., 2016; Oberhofer et al., 2010).

3.2 | Architectural parameters

3.2.1 | Fibre bundle length

Within the 30 identified studies, 13 measured FBL (Barber et al., 2017; Cenni et al., 2018b; Chen et al., 2018; D'Souza et al., 2019; Kawano et al., 2018; Kruse et al., 2018; Legerlotz et al., 2010; Malaiya et al., 2007; Mathewson et al., 2015; Mohagheghi et al., 2008; Morse et al., 2008; Shortland et al., 2002; Stephensen et al., 2012). In all but one paper, FBL measurements were performed using 2D B-mode ultrasound methods, with the other modality being MRI using DTI sequencing (D'Souza et al., 2019) (Table 3).

Most studies (as with the remaining architectural parameters) focussed on the architectural measurements of MG (Cenni et al., 2018b; D'Souza et al., 2019; Kawano et al., 2018; Kruse et al., 2018; Malaiya et al., 2007; Shortland et al., 2002), although a few studies had measurements for LG and SOL (Barber et al., 2017; Chen et al., 2018; Mathewson et al., 2015; Morse et al., 2008; Stephensen et al., 2012). Chen et al. (2018) was the only study to record measurements for all muscles of the *m. triceps surae*, showing LG with the highest

TABLE 3 FBL and PA measurements of the *m. triceps surae* in typically developing children, with studies ordered by ascending mean age of participants

Study	Age (years) Mean ± SD (range)	Number of participants (m:f)	Imaging	Muscle	FBL (cm) Mean ± SD	PA(°) Mean ± SD	Ankle position
Chen et al. (2018)	4.8 ± 2.0	24 (12:12)	2DUS	MG	3.70 ± 0.48	15.4 ± 3.3	Resting/20° PF
				LG	4.51 ± 0.72	10.7 ± 2.0	
				SOL	4.09 ± 1.04	14.7 ± 3.6	
Kawano et al. (2018)	6.4 ± 1.3	27 (11:16)	2DUS	MG	3.14 ± 0.32	25.9 ± 3.2	Resting
					4.96 ± 0.92	15.1 ± 2.5	Max DF
Legerlotz et al. (2010)	6.6 ± 2.3	21 (12:8)	2DUS	G	4.12 ± 0.62	15.7 ± 1.8	90°
					2.97 ± 0.41	21.5 ± 3.3	Max PF
Shortland et al. (2002)	7.8 (7–11)	5 (3:2)	2DUS	MG	4.49 ± 1.44	16.8 ± 2.9	0° PF
					4.1 ± 1.02	19.2 ± 4.2	15° PF
					3.61 ± 0.63	21.4 ± 3.4	30° PF
Wren et al. (2010)	8.8 ± 2.3	21 (7:14)	2DUS	MG	–	17.9 ± 2.5	Resting PF
Mohagheghi et al. (2008)	9.1 ± 2.3 (4–14)	50 (20:30)	2DUS	MG	4.2 ± 0.5	–	Resting (–18)
				LG	4.9 ± 0.6	–	
Malaiya et al. (2007)	9.5 (4–13)	15 (6:9)	2DUS	MG	4.9 ± 0.4	17.0 ± 1.9	Resting
					4.5 ± 0.7	15.8 ± 1.2	Max DF
Stephensen et al. (2012)	9.9 ± 1.3	19 (19:0)	2DUS	LG	5.63 ± 1.02	15.83 ± 4.21	40° PF
Barber et al. (2017)	10 ± 2.1	10	2DUS	MG	5.02 ± 0.75	–	–
				SOL	3.66 ± 0.72	–	–
Cenni et al. (2018b)	10.5 ± 2.6	11 (7:4)	3DUS	MG	2.92 ± 0.41	27.3 ± 2.1	Max PF
					3.81 ± 0.53	22.3 ± 2.5	50% ROM
					4.56 ± 0.58	19.2 ± 2.0	Max DF
			2DUS	MG	3.13 ± 0.46	24.9 ± 6.6	Max PF
					4.45 ± 0.92	19.7 ± 3.3	50% ROM
					5.43 ± 0.92	17.2 ± 3.2	Max DF
Morse et al. (2008)	10.9 ± 0.3	11 (11:0)	2DUS	LG	7.01 ± 0.79	10.8 ± 2.5	Resting
					4.2 ± 0.8	16.6 ± 4.6	Max PF
D'Souza et al. (2019)	11.2 ± 3.6 (5–18)	20 (13:7)	MRI	MG	3.87 ± 0.68	25.6 ± 3.6	Resting
Kruse et al. (2018)	11.3 ± 2.5	12 (5:7)	2DUS	MG	4.4 ± 0.8	18.1 ± 2.7	Resting
Mathewson et al. (2015)	12.4 ± 3.4	21 (10:11)	2DUS	SOL	3.5 ± 0.9	–	30° PF

Abbreviations: DF, dorsiflexion; G, gastrocnemius; LG, lateral gastrocnemius; MG, medial gastrocnemius; PF, plantar flexion; ROM, range of motion; SOL, soleus.

FBL and MG with the lowest for a given joint position (Chen et al., 2018). Mohagheghi et al. (2008) also showed that the FBL of LG was greater than that of MG (Mohagheghi et al., 2008).

Results across studies were variable, and it was difficult to compare studies across muscles and different ages due to the dependence of FBL on joint position. The parameters have been recorded as various degrees of plantarflexion (PF) and dorsiflexion (DF). Joint position acts as a major confounder when comparing the results of similar studies investigating FBL; hence it has been included in Table 3. A meta-regression was performed demonstrating a non-significant relationship between MG FBL and age in the identified studies (Figure 4) (Barber et al., 2017; Cenni et al., 2018b; Chen et al., 2018; D'Souza et al., 2019; Kawano et al., 2018; Kruse et al., 2018; Malaiya et al., 2007; Mohagheghi et al., 2008; Shortland et al., 2002).

3.2.2 | Pennation angle

Eleven studies examined PA (Cenni et al., 2018b; Chen et al., 2018; D'Souza et al., 2019; Kawano et al., 2018; Kruse et al., 2018; Legerlotz et al., 2010; Malaiya et al., 2007; Morse et al., 2008; Shortland et al., 2002; Standring, 2016; Wren et al., 2010) with ten using a 2D ultrasound system, and one utilising a DTI MRI sequence (Table 3).

A meta-regression was performed demonstrating a non-significant relationship between PA and age in MG among the identified studies (Figure 4) (Cenni et al., 2018b; Chen et al., 2018; D'Souza et al., 2019; Kawano et al., 2018; Kruse et al., 2018; Malaiya et al., 2007; Shortland et al., 2002; Wren et al., 2010).

3.2.3 | Muscle volume

Of the 15 studies, most have assessed MV using 3DUS (Barber et al., 2011a, 2011b, 2016; Malaiya et al., 2007; Obst et al., 2017; Schless et al., 2018, 2019a, 2019b; Willerslev-Olsen et al., 2018) and MRI (D'Souza et al., 2019; Herskind et al., 2016; Morse et al., 2008; Oberhofer et al., 2010; Pitcher et al., 2018; Vanmechelen et al., 2018). Equations have also been trialled to estimate MV based on easily obtainable measures such as aCSA and muscle length (ML) (Albracht et al., 2008; Mersmann et al., 2014) using 2DUS. Estimating MV is based on the equation MV = aCSAaverage × ML, where average aCSA (aCSAaverage) of a muscle is determined by the product of the maximum aCSA and a muscle form factor. The form factor is muscle-specific and considers the non-uniform cross-section of the muscle along its length (Vanmechelen et al., 2018).

Eleven studies assessed the morphology of the MG in isolation (Barber et al., 2011a, 2011b, 2016; D'Souza et al., 2019; Herskind et al., 2016; Malaiya et al., 2007; Morse et al., 2008; Oberhofer et al., 2010; Obst et al., 2017; Pitcher et al., 2018; Schless et al., 2018, 2019a, 2019b; Vanmechelen et al., 2018; Willerslev-Olsen et al., 2018) (Table 4). As would be expected, the average MV of the MG muscle appears to be larger within older age groups, for example, there was a mean MV of 14.1 ml at 1.4 years (Willerslev-Olsen et al., 2018), compared with a mean MV of 223 ml at 18 years (Barber et al., 2011b); however, no formal statistical comparisons could be made.

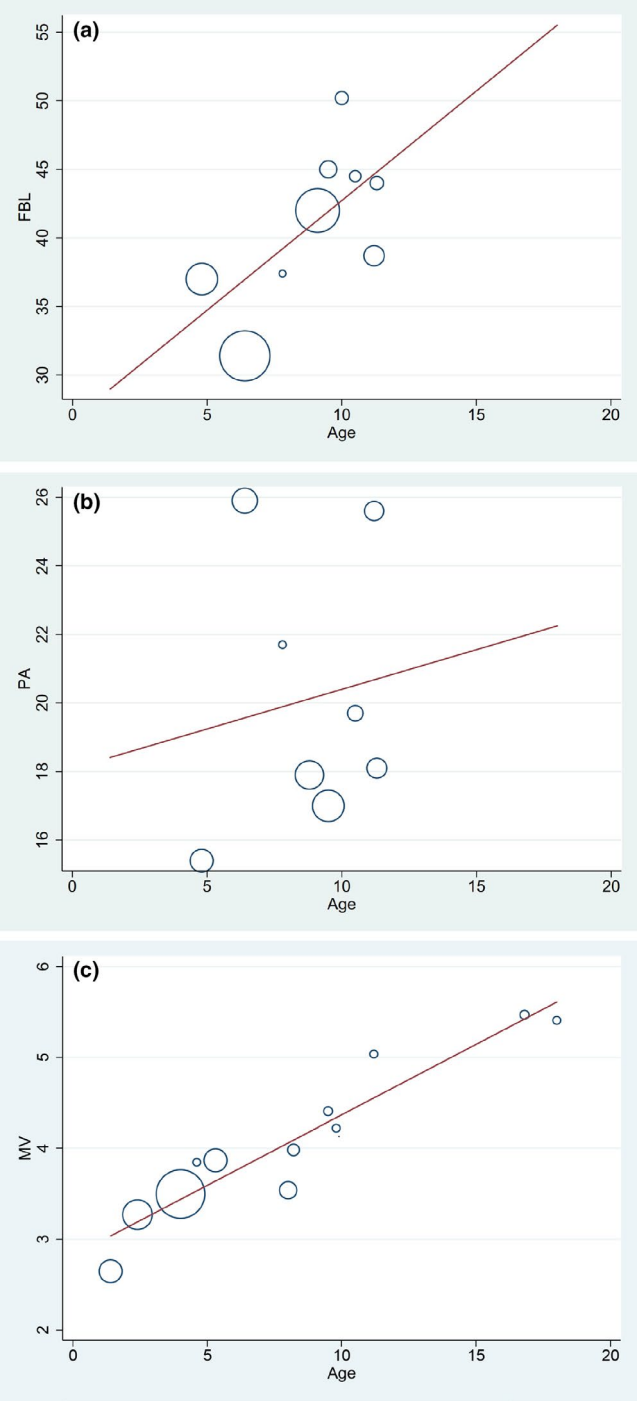

FIGURE 4 (a) Meta-regression of MG FBL (mm) as the dependent variable and age (years) as the independent variable. (b) Meta-regression of MG PA (degrees) as the dependent variable and age (years) as the independent variable. (c) Meta-regression of MG MV (log ml) as the dependent variable and age (years) as the independent variable

TABLE 4 MV measurements of the *m. triceps surae* in typically developing children, with studies ordered by ascending mean age of participants

Study	Age (years) Mean ± SD (range)	Number of participants (m:f)	Imaging	Muscle	MV (mL) Mean ± SD
Willerslev-Olsen et al. (2018)	1.4 ± 1.1	45	3DUS	MG	14.1 ± 9.1
Herskind et al. (2016)	2.4	101 (47/54)	MRI	MG	26.3 ± 12.9
Barber et al. (2011a)	4 ± 1.2	20 (11/9)	3DUS	MG	33 ± 2
Obst et al. (2017)	4.6 ± 2.4	10 (5/5)	3DUS	MG	46.8 ± 23.7
Barber et al. (2016)	5.3 ± 1.3	78 (40/38)	3DUS	MG	47.8 ± 17.9
Pitcher et al. (2018)	8 ± 1.4[a]	19	MRI	MG LG SOL	34.4[a] 22.1[a] 101.9[a]
Schless et al. (2018)	8.2 ± 1.5	15 (6/9)	3DUS	MG	53.6 ± 12.2
Schless et al. (2019b)	9.9[a] 7.10–11.6	67 (43/24)	3DUS	MG	62 (49.7–81.8)[b]
Malaiya et al. (2007)	4–13	15 (6/9)	3DUS	MG	82.1 ± 27.3
Schless et al. (2018)	9.8 ± 2.4	10 (8/2)	3DUS	MG	68.1 ± 20.6
Oberhofer et al. (2010)	10.2 ± 1.2	5	MRI	LG+MG SOL	149.6 ± 29.92 187 ± 37.4
Morse et al. (2008)	10.9 ± 0.3	11 (11/0)	MRI	LG	64.5 ± 18.9
D'Souza et al. (2019)	11.2 ± 3.6 (5–18)	20	MRI	MG	153.9 ± 74.60
Vanmechelen et al. (2018)	16.8 ± 3.3 (10.6–23.2)	23 (16/7)	MRI	MG SOL	237 ± 57 428 ± 107
Barber et al. (2011b)	18 ± 2 (15–20)	10 (5/5)	3DUS	MG	223 ± 21

Abbreviations: LG, lateral gastrocnemius; MG, medial gastrocnemius; SOL, soleus.

[a]Data expressed as median ± median absolute deviation.

[b]Data expressed as median ± inter quartile range.

MRI and 3DUS have both been utilised to measure in vivo muscle volume of the *m. triceps surae* in 6 and 9 studies respectively.

A meta-regression was performed demonstrating the positive relationship between MV and age in MG among the identified studies (Figure 4) (Barber et al., 2011a, 2011b, 2016; D'Souza et al., 2019; Herskind et al., 2016; Obst et al., 2017; Pitcher et al., 2018; Schless et al., 2018, 2019a, 2019b; Vanmechelen et al., 2018; Willerslev-Olsen et al., 2018).

3.2.4 | Physiological cross-sectional area

Four studies assessed pCSA (n =3 MG, n = 1 LG), which demonstrated an apparent increase in MG from age 4 to 18-years-old (Table 5) (Barber et al., 2011a, 2011b; D'Souza et al., 2019; Morse et al., 2008).

3.3 | Reliability

3.3.1 | 2DUS

Of the 30 studies included within this review, only three included reliability testing of the 2DUS technique (Cenni et al., 2018b; Legerlotz et al., 2010; Stephensen et al., 2012). Legerlotz et al. (2010) assessed the intra-acquirer reliability of FBL and PA measurements from two images that were captured during the same scanning session (Table 6) (Legerlotz et al., 2010). Measurements were taken with the ankle in maximum plantarflexion and at 90 degrees neutral. Reliability was assessed using the intra-class correlation coefficient (ICC), with all ICCs ranging from good to excellent (0.868–0.983). For the purposes of this review, an ICC of over 0.7 indicates good reliability, while a result above 0.9 indicates excellent reliability.

Cenni et al. (2018b) assessed intra-acquirer reliability at three different ankle positions (Table 7) (Cenni et al., 2018b). While most ICCs were good to excellent, the reliability of PA measurements at 50% range of motion and maximum dorsiflexion was significantly lower. In this study, the reliability of 2D and 3D ultrasound were compared for FBL and PA measurements, with the 3D technique being determined as more reliable. This was attributed to the higher acquisition accuracy required when using 2DUS, from which architectural measurements are calculated from a single image. Stephensen et al. (2012) assessed the test–retest reliability of 2DUS for assessment of LG FBL and PA and found excellent ICCs (ranging from 0.99 to 1.00).

3.3.2 | 3DUS

Of the 30 studies included within this review, only two included reliability testing of 3DUS assessment of *m. triceps surae* of typically developing children (Cenni et al., 2018a, 2018b), one testing the reliability of FBL and PA measurements in different joint positions (Cenni et al., 2018b), and the other assessing the reliability of MV calculations (Cenni et al., 2018a). Both reliability measurements were quantified using the ICC.

Cenni et al. (2018b) assessed the inter-acquirer reliability of freehand 3DUS for measurement of FBL and PA at several joint positions (Cenni et al., 2018b). For FBL, ICCs were excellent (0.914–0.952), while PA ICCs were good (0.719–0.852) across different joint positions.

Cenni et al. (2018a) included various types of reliability, including inter-acquirer, intra-acquirer and inter-processor reliability testing of MV, with all reported ICCs being excellent (0.986–0.994). There was no intra-processor reliability which remains a gap in the current literature.

TABLE 5 pCSA measurements of the *m. triceps surae* in typically developing children, with studies ordered by ascending mean age of participants

Study	Age (years) (mean ± SD)	Number of participants (m:f)	Imaging	Muscle	pCSA (cm^2)
Barber et al. (2011a)	4 (2–5)	20 (11/9)	3D US	MG	7.3 ± 0.5
Morse et al. (2008)	10.9 ± 0.3	11 (11/0)	2D US	LG	15.5 ± 3.2
D'Souza et al. (2019)	11.2 ± 3.6 (5–18)	20 (13/7)	DTI	MG	38.6 ± 12.9
Barber et al. (2011b)	18 ± 2 (15–20)	10 (5/5)	3D US	MG	53 ± 5

Abbreviations: LG, lateral gastrocnemius; MG, medial gastrocnemius; SOL, soleus.

3.4 | MRI

One study was identified that included reliability analyses for MRI in assessing *m. triceps surae* muscle volume (Noble et al., 2017). Inter-processor reliability compared two processors and found excellent reliability of muscle volume segmentation for MG and SOL in children with a mean age of 16.8 years, with ICCs of 0.984 and 0.997, respectively. No studies have assessed the reliability of DTI sequence measurements in children.

4 | DISCUSSION

The goal of this review was to explore the methodologies utilised in the investigation of *m. triceps surae* architecture in typically developing children. Most of these studies investigated MG as the muscle of interest, with an under-representation of LG and SOL in

TABLE 6 FBL and PA reliability with 2DUS in left and right gastrocnemius

Study	Age (years ± SD)	Number of participants	Architectural parameter	Intra-acquirer reliability (ICC)			
				Left gastrocnemius		Right gastrocnemius	
				90° neutral	Max PF	90° neutral	Max PF
Legerlotz et al. (2010)	6.3 ± 2.3		FBL	0.887	0.918	0.900	0.868
			PA	0.876	0.960	0.876	0.942

Abbreviations: DF, Dorsiflexion; ICC, intra-class correlation coefficient; PF, plantar flexion; ROM, range of motion.

TABLE 7 MG FBL and PA reliability with 2DUS in different ankle positions

Study	Age (years ± SD)	Number of participants	Architectural parameter	Intra-acquirer reliability (ICC)		
				Max PF	50% ROM	Max DF
Cenni et al. (2018b)	10.5 ± 2.6	11 (7/4)	FBL	0.694	0.917	0.802
			PA	0.963	0.210	0.663

Abbreviations: DF, dorsiflexion; ICC, intra-class correlation coefficient; PF, plantar flexion; ROM, range of motion.

the results. Three imaging modalities were identified across all the identified studies: 2DUS, 3DUS and MRI. Within each of these techniques, there was marked variation in methodology between studies, namely in the acquisition process. These modalities were used to differentially assess aspects of the *m. triceps surae* architecture, including FBL, PA, MV and pCSA. While the results of this review show possible changes in MV and pCSA with age from 1 to 18 years old, there were no similar, discernible trends identified with FBL and PA. This discrepancy may be due to methodological variations between studies, creating difficulty in making direct comparisons. No studies assessed the *m. triceps surae* architecture in the first year of life. Finally, only five studies have been conducted investigating the reliability of measurements across all three of the described techniques. Additionally, no studies have assessed intra-processor reliability. This review provides insight into the current literature concerning the assessment of the *m. triceps surae* architectural parameters in typically developing children. These data have the potential to inform future research in skeletal muscle architecture, specifically relating to the use of imaging modalities to acquire measurements of internal morphology, how they are used and the populations of interest.

4.1 | 2DUS

2DUS has been primarily utilised to investigate FBL and PA in typically developing children.

Based on pulled data from studies included in this review, no significant correlation could be determined between age and FBL or PA. However, limitations in study designs and the variation in participant joint positioning for measurements (with both FBL and PA measurements being highly dependent on this variable) make accurate comparisons challenging. Studies reporting 'resting' joint angle may add further complications for standardised comparisons, and the complete absence of longitudinal studies further exacerbates efforts to establish an age-dependent relationship.

External to this review, several studies investigating differences between child and adult muscle architecture have asserted that FBL increases from childhood (Kannas et al., 2010; O'Brien et al., 2010). Bénard et al. (2011) demonstrated an increase in MG FBL from age 5 to 12 years, with no significant change in PA. In contrast, Binzoni et al. (2001) and Kannas et al. (2010) reported an increase in PA from infancy to adolescence. Shortland et al. (2002) reported similar changes but were only significant at one ankle angle, 30 degrees plantarflexion.

No differences in architecture can be drawn between male and female participants across the included literature. While the number of male/female participants has been included, no significant differences in architectural parameters between genders have been identified at present, supported by a single study by O'Brien et al. (2010). Future research analysing the potential of sexual dimorphism in *m. triceps surae* architecture may be required to contribute to a complete understanding of skeletal muscle development.

2D ultrasound does have several limitations that have been described in the literature (Bénard et al., 2009; Bolsterlee et al., 2016a; Klimstra et al., 2007; Martin et al., 2001). Inconsistent probe orientation to visualise the imaging plane between studies may result in measurement errors (Bénard et al., 2009; Bolsterlee et al., 2016b; Klimstra et al., 2007). The FBL and PA vary at different joint angles (Klimstra et al., 2007; Narici et al., 1996) and states of contraction (Maganaris et al., 1998; Martin et al., 2001; Narici et al., 1996). Finally, the measurement sites of the muscles of interest were also different between studies (Agur et al., 2003; Bradshaw et al., 2020). Together this makes 2DUS a highly operator and methodology dependent method of acquiring muscle architectural parameter measurements.

Alongside the described limitations and challenges faced by ultrasound for measurement of muscle architecture, reliability analyses are few. A systematic review by Kwah et al. (2013) demonstrates several studies investigating the reliability of 2DUS for the measurement of FBL and PA. These studies, along with several published since, did not meet the inclusion criteria but highlighted good to excellent reliability of 2DUS within their respective study populations (Aeles et al., 2017; Gillett et al., 2013; Kannas et al., 2010; König et al., 2014; Mcmahon et al., 2016; Mohagheghi et al., 2007; Raj et al., 2012).

Excessive pressure application via an ultrasound transducer can influence the underlying muscle architecture and is a consideration when utilising 3DUS for muscle volume assessment (as will be discussed). Hence, this influence may translate to 2DUS use for investigation of FBL and PA. However, as reported by Bolsterlee et al. (2016a), only superficial pennation angle is affected by excessive probe pressure, while measurements of deep pennation angle and fibre bundle length are not significantly influenced.

Finally, there are no studies assessing the architecture of the *m. triceps surae* in healthy infants. It is well known that skeletal muscle adapts to meet the evolving functional demands of daily life. With these gaps in the literature, however, there remain many unknowns regarding the changes in *m. triceps surae* architecture from infancy to adolescence.

4.2 | 3DUS

Freehand 3DUS is becoming an increasingly popular method of investigating *in vivo m. triceps surae* architecture, particularly those with cerebral palsy (CP) (Barber et al., 2019; Malaiya et al., 2007; Schless et al., 2019b). 3DUS has almost exclusively been used for MV assessment. Comparing the current range of studies that have been performed reveals that the muscle volume of MG tends to increase with age from childhood to adolescence. Despite the relatively limited data available on LG and SOL muscle volume measurements, there is an apparent increase with age. It is generally accepted that muscle size increases in response to aging throughout childhood (Kanehisa et al., 1995; Malina, 1975). Specific studies demonstrating the typical growth of the *m. triceps surae* muscles are scarce (Morse et al., 2008; Weide et al., 2015). Morse et al. (2008) compared muscle size in typically developing

children with that of adults, and found that the adult LG had significantly greater MV and pCSA.

Like muscle volume, the pCSA exhibits a marked increase with age. The observed increase in pCSA with age is likely a function of the increasing functional demands faced by the *m. triceps surae*. Given its role within standing and walking, the ability of *m. triceps surae* to carry out its function is dependent on generating sufficient force to support an individual's body weight. Hence, as age and weight increase together throughout childhood to adolescence, the demands on the *m. triceps surae* increase, contributing to a mechanical stimulus for the muscle to grow in size and force-generating capacity (Bénard et al., 2011; Binzoni et al., 2001; Weide et al., 2015). Additionally, bone lengthening in response to increases in height and leg length likely produces muscle lengthening and growth (Weide et al., 2015), contributing to a gain in muscle volume and pCSA. As a primary indicator of the relative maximum force that can be generated by a muscle and the number of sarcomeres in parallel, this increase likely reflects an increase in the contractile force that may be generated by the MG.

Several studies have demonstrated that 3DUS produces reliable and reproducible results of *in vivo* muscle volume (Barber et al., 2009, 2019; Cenni et al., 2016; Noorkoiv et al., 2019), with good agreement to results obtained using MRI (Barber et al., 2009; Noorkoiv et al., 2019). In contrast, only one of these reliability studies has been conducted in typically developing children (Cenni et al., 2018a).

There are a few considerations when utilising 3DUS. Two primary sources of error exist when quantifying muscle volume with this technique: acquisition and segmentation error. Acquisition errors occur because of methodological issues relating to the scanning and acquiring of ultrasound data. Careful consideration of these issues is required for the method to be reliable. Firstly, tissue compression resulting from excessive pressure from the transducer can cause deformation of muscles and alterations in muscle volume calculations (Barber et al., 2009; Cenni et al., 2018a; Raiteri et al., 2016). Studies have trialled several methods to limit the deformation of the muscle by the transducer, including the use of a water bath (Barber et al., 2009), excessive acoustic gel (Barber et al., 2016; Obst et al., 2017; Schless et al., 2018, 2019b; Willerslev-Olsen et al., 2018) and most recently, a curved gel pad attached to the transducer section (Cenni et al., 2018c; Noorkoiv et al., 2019).

Other methodological considerations during acquisition include moving the transducer at a relatively constant velocity during a sweep and holding the probe perpendicular to the skin to permit better image quality (Cenni et al., 2018a; MacGillivray et al., 2009).

Segmentation involves manually outlining muscles using the obtained 2D B-mode US images. The corresponding borders are interpolated to generate a 3D mesh of a muscle from which muscle volume can be quantified. Errors during the segmentation process ultimately affect muscle volume results and come in multiple forms (Barber et al., 2019; Noorkoiv et al., 2019). Firstly, as the outlined borders are linearly interpolated, if too few images are segmented, muscle volume may be underestimated (Cenni et al., 2018a). Image quality can have a noticeable impact on segmentation regarding the accurate identification of muscle borders (Barber et al., 2019; Noorkoiv et al., 2019). More significant variability between individual processors has been reported previously (Barber et al., 2019).

4.3 | MRI

Only one study has been conducted that reported on the reliability of MRI assessment of in vivo *m. triceps surae* muscle volume in typically developing children (Noble et al., 2017). While other studies exist assessing the reproducibility of MRI results, analyses of typically developing muscles may not be reported, or grouped with analyses of pathological muscles (Barber et al., 2019; Herskind et al., 2016). The sole included study only investigated inter-processor reliability and found excellent results for both MG and SOL. MRI also presents several significant considerations that limit its overall utility, including its high cost and long scanning times during which participants must remain still.

4.4 | Limitations of the review

This review has several limitations that must be discussed. Only specific architectural parameters (FBL, PA, MV and pCSA) were examined. Other morphological and architectural measurements, such as aCSA, muscle length and stiffness, have been examined but were omitted. Regarding age-dependent changes in architecture, the MG was exclusively discussed and analysed due to the relative scarcity of studies reporting data on LG and SOL. This review exclusively examined architecture within a specific age range; thus, no conclusions can be made regarding the state of research in adults. Additionally, limiting this review to original, English publications has the potential to exclude potentially viable research within conference proceedings and short communications. All studies meeting the inclusion criteria were added to this review, regardless of study quality. This creates the potential for low-quality methodology to influence the overall results and conclusions. Furthermore, only studies that had reported on solely typically developing data were included; hence further elucidations could be made with normative typically developing data presented within studies of clinical populations.

5 | CONCLUSION

Due to the limitations inherent within each *in vivo* imaging modality and wide variation in study methodologies, interpretations of the data are challenging. Concentrated efforts to minimise confounding variables and detailed, consistent methodology may assist with the production of directly comparable results. Likewise, longitudinal studies following the changes in muscle parameters over time may facilitate a more complete understanding of muscle development within specific developmental age bands (such as childhood

to adolescence). Finally, relative to the number of studies utilising *in vivo* muscle imaging to acquire measurements of muscle morphology, fewer have investigated the feasibility and reliability of the methods used. Reliability is an essential consideration for the future that has been underreported at present. Similar results were observed in a recent scoping review evaluating studies investigating the architecture of children with CP (Williams et al., 2020). Overall, non-invasive imaging modalities have a clear and definable role in quantifying *m. triceps surae* muscle architecture in children and adolescents. Explicit methodological descriptions and efforts to minimise confounding variables must be a cornerstone of muscle architecture investigation in future studies. Given the relative lack of conclusions that can be drawn thus far, further investigation is required to determine the time course of typical *m. triceps surae* development. This will assist in the formation of a model of muscle development, and its relationship with changing physical demands that occur throughout childhood.

DATA AVAILABILITY STATEMENT

n/a.

ORCID

Matthew Bell https://orcid.org/0000-0002-0072-3327
Sîan A. Williams https://orcid.org/0000-0002-4907-7477
Ali Mirjalili https://orcid.org/0000-0002-1599-3573

REFERENCES

Aeles, J., Lichtwark, G.A., Lenchant, S. & Vanlommel, L. (2017) Information from dynamic length changes improves reliability of static ultrasound fascicle length measurements. *PeerJ*, 5, 1–18.

Agur, A.M., Ng-Thow-Hing, V., Ball, K.A., Fiume, E. & McKee, N.H. (2003) Documentation and three-dimensional modelling of human soleus muscle architecture. *Clinical Anatomy*, 16(4), 285–293.

Albracht, K., Arampatzis, A. & Baltzopoulos, V. (2008) Assessment of muscle volume and physiological cross-sectional area of the human triceps surae muscle in vivo. *Journal of Biomechanics*, 41(10), 2211–2218.

Barber, L., Alexander, C., Shipman, P., Boyd, R., Reid, S. & Elliott, C. (2019) Validity and reliability of a freehand 3D ultrasound system for the determination of triceps surae muscle volume in children with cerebral palsy. *Journal of Anatomy*, 234(3), 384–391.

Barber, L., Barrett, R. & Lichtwark, G. (2009) Validation of a freehand 3D ultrasound system for morphological measures of the medial gastrocnemius muscle. *Journal of Biomechanics*, 42(9), 1313–1319.

Barber, L., Barrett, R. & Lichtwark, G. (2011) Passive muscle mechanical properties of the medial gastrocnemius in young adults with spastic cerebral palsy. *Journal of Biomechanics*, 44(13), 2496–2500.

Barber, L., Carty, C., Modenese, L., Walsh, J., Boyd, R. & Lichtwark, G. (2017) Medial gastrocnemius and soleus muscle-tendon unit, fascicle, and tendon interaction during walking in children with cerebral palsy. *Developmental Medicine and Child Neurology*, 59(8), 843–851.

Barber, L., Hastings-Ison, T., Baker, R., Barrett, R. & Lichtwark, G. (2011) Medial gastrocnemius muscle volume and fascicle length in children aged 2 to 5years with cerebral palsy. *Developmental Medicine and Child Neurology*, 53(6), 543–548.

Barber, L.A., Read, F., Lovatt Stern, J., Lichtwark, G. & Boyd, R.N. (2016) Medial gastrocnemius muscle volume in ambulant children with unilateral and bilateral cerebral palsy aged 2 to 9 years. *Developmental Medicine and Child Neurology*, 58(11), 1146–1152.

Bénard, M.R., Becher, J.G., Harlaar, J., Huijing, P.A. & Jaspers, R.T. (2009) Anatomical information is needed in ultrasound imaging of muscle to avoid potentially substantial errors in measurement of muscle geometry. *Muscle and Nerve*, 219(3), 388–402.

Bénard, M.R., Harlaar, J., Becher, J.G., Huijing, P.A. & Jaspers, R.T. (2011) Effects of growth on geometry of gastrocnemius muscle in children: a three-dimensional ultrasound analysis. *Journal of Anatomy*, 219(3), 388–402.

Binzoni, T., Bianchi, S., Hanquinet, S., Kaelin, A., Sayegh, Y., Dumont, M. et al. (2001) Human gastrocnemius medialis pennation angle as a function of age: from newborn to the elderly. *Journal of Physiological Anthropology and Applied Human Science*, 20(5), 293–298.

Bolsterlee, B., Finni, T., D'Souza, A., Eguchi, J., Clarke, E.C. & Herbert, R.D. (2018) Three-dimensional architecture of the whole human soleus muscle in vivo. *PeerJ*, 6, e4610.

Bolsterlee, B., Gandevia, S.C. & Herbert, R.D. (2016) Effect of transducer orientation on errors in ultrasound image-based measurements of human medial gastrocnemius muscle fascicle length and pennation. *PLoS One*, 11(6), e0157273.

Bolsterlee, B., Gandevia, S.C. & Herbert, R.D. (2016) Ultrasound imaging of the human medial gastrocnemius muscle: How to orient the transducer so that muscle fascicles lie in the image plane. *Journal of Biomechanics*, 49(7), 1002–1008.

Bradshaw, L., Brienhorst, E., Stott, N.S., Agur, A.M.R. & Mirjalili, S.A. (2020) The architecture of the 6-month-old gastrocnemius: a 3D volumetric study. *European Journal of Anatomy*, 24(6), 491–499.

Brink, Y. & Louw, Q.A. (2012) Clinical instruments: reliability and validity critical appraisal. *Journal of Evaluation in Clinical Practice*, 18(6), 1126–1132.

Cenni, F., Bar-On, L., Schless, S.H., Kalkman, B., Aertbelien, E., Bruyninckx, H. et al. (2018) Medial gastrocnemius muscle-tendon junction and fascicle lengthening across the range of motion analyzed in 2-D and 3-D ultrasound images. *Ultrasound in Medicine and Biology*, 44(12), 2505–2518.

Cenni, F., Monari, D., Desloovere, K., Aertbeliën, E., Schless, S.H. & Bruyninckx, H. (2016) The reliability and validity of a clinical 3D freehand ultrasound system. *Computer Methods and Programs in Biomedicine*, 136, 179–187.

Cenni, F., Schless, S.H., Bar-On, L., Aertbeliën, E., Bruyninckx, H., Hanssen, B. et al. (2018) Reliability of a clinical 3D freehand ultrasound technique: Analyses on healthy and pathological muscles. *Computer Methods and Programs in Biomedicine*, 156, 97–103.

Cenni, F., Schless, S.H., Monari, D., Bar-On, L., Aertbeliën, E., Bruyninckx, H. et al. (2018) An innovative solution to reduce muscle deformation during ultrasonography data collection. *Journal of Biomechanics*, 77, 194–200.

Chelly, S.M. & Denis, C. (2001) Leg power and hopping stiffness: relationship with sprint running performance. *Medicine and Science in Sports and Exercise*, 33(2), 326–333.

Chen, Y., He, L., Xu, K., Li, J., Guan, B. & Tang, H. (2018) Comparison of calf muscle architecture between Asian children with spastic cerebral palsy and typically developing peers. *PLoS One*, 13(1), e0190642.

D'Souza, A., Bolsterlee, B., Lancaster, A. & Herbert, R.D. (2019) Muscle architecture in children with cerebral palsy and ankle contractures: an investigation using diffusion tensor imaging. *Clinical Biomechanics*, 68, 205–211.

Finanger, E.L., Russman, B., Forbes, S.C., Rooney, W.D., Walter, G.A. & Vandenborne, K. (2012) Use of skeletal muscle MRI in diagnosis and monitoring disease progression in duchenne muscular dystrophy. *Physical Medicine and Rehabilitation Clinics of North America*, 23(1), 1–10.

Gans, C. & de Vree, F. (1987) Functional bases of fiber length and angulation in muscle. *Journal of Morphology*, 192(1), 63–85.

Gillett, J.G., Barrett, R.S., Lichtwark, G.A., Gillett, J.G., Barrett, R.S. & Reliability, G.A.L. (2013) Computer methods in biomechanics and

biomedical engineering reliability and accuracy of an automated tracking algorithm to measure controlled passive and active muscle fascicle length changes from ultrasound. *Computer Methods in Biomechanics and Biomedical Engineering*, 16(6), 678–687.

Herskind, A., Ritterband-Rosenbaum, A., Willerslev-Olsen, M., Lorentzen, J., Hanson, L., Lichtwark, G. et al. (2016) Muscle growth is reduced in 15-month-old children with cerebral palsy. *Developmental Medicine and Child Neurology*, 58(5), 485–491.

Hsu, P.W., Prager, R.W., Gee, A.H. & Treece, G.M. (2009) Freehand 3D ultrasound calibration: a review. In: *Advanced imaging in biology and medicine: technology, software environments, applications*, pp. 47–84.

Kanehisa, H., Yata, H., Ikegawa, S. & Fukunaga, T. (1995) A cross-sectional study of the size and strength of the lower leg muscles during growth. *European Journal of Applied Physiology and Occupational Physiology*, 72(1), 150–156.

Kannas, T., Kellis, E. & Arampatzi, F. (2010) Medial gastrocnemius architectural properties during isometric contractions in boys and men. *Pediatric Exercise Science*, 38, 152–164.

Kawano, A., Yanagizono, T., Kadouchi, I., Umezaki, T. & Chosa, E. (2018) Ultrasonographic evaluation of changes in the muscle architecture of the gastrocnemius with botulinum toxin treatment for lower extremity spasticity in children with cerebral palsy. *Journal of Orthopaedic Science*, 23(2), 389–393.

Klimstra, M., Dowling, J., Durkin, J.L. & MacDonald, M. (2007) The effect of ultrasound probe orientation on muscle architecture measurement. *Journal of Electromyography and Kinesiology*, 17(4), 504–514.

König, N., Cassel, M., Intziegianni, K. & Mayer, F. (2014) Inter-rater reliability and measurement. *Journal of Ultrasound in Medicine*, 3, 769–777.

Kruse, A., Schranz, C., Tilp, M. & Svehlik, M. (2018) Muscle and tendon morphology alterations in children and adolescents with mild forms of spastic cerebral palsy. *BMC Pediatrics*, 18(1).

Kwah, L.K., Pinto, R.Z., Diong, J. & Herbert, R.D. (2013) Reliability and validity of ultrasound measurements of muscle fascicle length and pennation in humans: a systematic review. *Journal of Applied Physiology*, 114(6), 761–769.

Lee, D., Li, Z., Sohail, Q.Z., Jackson, K., Fiume, E. & Agur, A. (2015) A three-dimensional approach to pennation angle estimation for human skeletal muscle. *Computer Methods in Biomechanics and Biomedical Engineering*, 18(13), 1474–1484.

Legerlotz, K., Smith, H.K. & Hing, W.A. (2010) Variation and reliability of ultrasonographic quantification of the architecture of the medial gastrocnemius muscle in young children. *Clinical Physiology and Functional Imaging*, 30(3), 198–205.

Lichtwark, G. (2017) Ultrasound technology for examining the mechanics of the muscle, tendon, and ligament. In: *Handbook of human motion*, pp. 1–20.

Lieber, R.L. (2011) Skeletal muscle structure, function, and plasticity. *Skeletal Muscle Structure, Function, and Plasticity*, 1–304.

Lieber, R.L. & Fridén, J. (2000) Functional and clinical significance of skeletal muscle architecture. *Muscle and Nerve*, 23(11), 1647–1666.

Lieber, R.L. & Ward, S.R. (2011) Skeletal muscle design to meet functional demands. *Philosophical Transactions of the Royal Society B: Biological Sciences*, 366(1570), 1466–1476.

MacGillivray, T.J., Ross, E., Simpson, H.A.H.R.W. & Greig, C.A. (2009) 3D Freehand Ultrasound for in vivo Determination of Human Skeletal Muscle Volume. *Ultrasound in Medicine and Biology*, 35(6), 928–935.

Maganaris, C.N., Baltzopoulos, V. & Sargeant, A.J. (1998) In vivo measurements of the triceps surae complex architecture in man: Implications for muscle function. *Journal of Physiology*, 512(2), 603–614.

Malaiya, R., McNee, A.E., Fry, N.R., Eve, L.C., Gough, M. & Shortland, A.P. (2007) The morphology of the medial gastrocnemius in typically developing children and children with spastic hemiplegic cerebral palsy. *Journal of Electromyography and Kinesiology*, 17(6), 657–663.

Malina, R. (1975) *Growth and development: the first twenty years in man*. Minneapolis: Burgess Publishing Company.

Martin, D.C., Medri, M.K., Chow, R.S., Oxorn, V., Leekam, R.N., Agur, A.M. et al. (2001) Comparing human skeletal muscle architectural parameters of cadavers with in vivo ultrasonographic measurements. *Journal of Anatomy*, 199(4), 429–434.

Mathewson, M.A., Ward, S.R., Chambers, H.G. & Lieber, R.L. (2015) High resolution muscle measurements provide insights into equinus contractures in patients with cerebral palsy. *Journal of Orthopaedic Research*, 33(1), 33–39.

Mcmahon, J., Turner, A. & Comfort, P. (2016) Within- and between-session reliability of medial gastrocnemius architectural properties. *Biology of Sport*, 33(2), 185–188.

Mersmann, F., Bohm, S., Schroll, A. & Arampatzis, A. (2014) Validation of a simplified method for muscle volume assessment. *Journal of Biomechanics*, 47(6), 1348–1352.

Mitsiopoulos, N., Baumgartner, R.N., Heymsfield, S.B., Lyons, W., Gallagher, D. & Ross, R. (1998) Cadaver validation of skeletal muscle measurement by magnetic resonance imaging and computerized tomography. *Journal of Applied Physiology*, 85(1), 115–122.

Mohagheghi, A.A., Khan, T., Meadows, T.H., Giannikas, K., Baltzopoulos, V. & Maganaris, C.N. (2007) Differences in gastrocnemius muscle architecture between the paretic and non-paretic legs in children with hemiplegic cerebral palsy. *Clinical Biomechanics*, 22(6), 718–724.

Mohagheghi, A.A., Khan, T., Meadows, T.H., Giannikas, K., Baltzopoulos, V. & Maganaris, C.N. (2008) In vivo gastrocnemius muscle fascicle length in children with and without diplegic cerebral palsy. *Developmental Medicine and Child Neurology*, 50(1), 44–50.

Moore, K.L., Dalley, A.F. & Agur, A.M.R. (2014) Clinically orientated anatomy 7e. In: *Clinically orientated anatomy*.

Morse, C.I., Smith, J., Denny, A., Tweedale, J. & Searle, N.D. (2015) Gastrocnemius medialis muscle architecture and physiological cross sectional area in adult males with Duchenne muscular dystrophy. *Journal of Musculoskeletal Neuronal Interactions*, 15(2), 154–160.

Morse, C.I., Tolfrey, K., Thom, J.M., Vassilopoulos, V., Maganaris, C.N. & Narici, M.V. (2008) Gastrocnemius muscle specific force in boys and men. *Journal of Applied Physiology*, 104(2), 469–474.

Murray, M.P., Guten, G.N., Baldwin, J.M. & Gardner, G.M. (1976) A comparison of plantar flexion torque with and without the triceps surae. *Acta Orthopaedica*, 47(1), 122–124.

Narici, M. (1999) Human skeletal muscle architecture studied in vivo by non-invasive imaging techniques: functional significance and applications. *Journal of Electromyography and Kinesiology*, 9(2), 97–103.

Narici, M.V., Binzoni, T., Hiltbrand, E., Fasel, J., Terrier, F. & Cerretelli, P. (1996) In vivo human gastrocnemius architecture with changing joint angle at rest and during graded isometric contraction. *Journal of Physiology*, 496(1), 287–297.

Neptune, R.R., Kautz, S.A. & Zajac, F.E. (2001) Contributions of the individual ankle plantar flexors to support, forward progression and swing initiation during walking. *Journal of Biomechanics*, 34(11), 1387–1398.

Noble, J.J., Chruscikowski, E., Fry, N.R.D., Lewis, A.P., Gough, M. & Shortland, A.P. (2017) The relationship between lower limb muscle volume and body mass in ambulant individuals with bilateral cerebral palsy. *BMC Neurology*, 17(1).

Noorkoiv, M., Theis, N. & Lavelle, G. (2019) A comparison of 3D ultrasound to MRI for the measurement and estimation of gastrocnemius muscle volume in adults and young people with and without cerebral palsy. *Clinical Anatomy*, 32(3), 319–327.

O'Brien, T.D., Reeves, N.D., Baltzopoulos, V., Jones, D.A. & Maganaris, C.N. (2009) Strong relationships exist between muscle volume, joint power and whole-body external mechanical power in adults and children. *Experimental Physiology*, 94(6), 731–738.

O'Brien, T.D.O., Reeves, N.D., Baltzopoulos, V., Jones, D.A. & Maganaris, C.N. (2010) Muscle–tendon structure and dimensions in adults and children. *Journal of Anatomy*, 216(5), 631–642.

Oberhofer, K., Stott, N.S., Mithraratne, K. & Anderson, I.A. (2010) Subject-specific modelling of lower limb muscles in children with cerebral palsy. *Clinical Biomechanics*, 25(1), 88–94.

Obst, S.J., Boyd, R., Read, F. & Barber, L. (2017) Quantitative 3-D ultrasound of the medial gastrocnemius muscle in children with unilateral spastic cerebral palsy. *Ultrasound in Medicine and Biology*, 43(12), 2814–2823.

Park, E.S., Sim, E., Rha, D.W. & Jung, S. (2014) Estimation of gastrocnemius muscle volume using ultrasonography in children with spastic cerebral palsy. *Yonsei Medical Journal*, 55(4), 1115–1122.

Pitcher, C.A., Elliott, C.M., Valentine, J.P., Stannage, K., Williams, S.A., Shipman, P.J. et al. (2018) Muscle morphology of the lower leg in ambulant children with spastic cerebral palsy. *Muscle and Nerve*, 58(6), 818–823.

Prager, R.W., Rohling, R.N., Gee, A.H. & Berman, L. (1998) Rapid calibration for 3-D freehand ultrasound. *Ultrasound in Medicine and Biology*, 24(6), 855–869.

Raiteri, B.J., Cresswell, A.G. & Lichtwark, G.A. (2016) Three-dimensional geometrical changes of the human tibialis anterior muscle and its central aponeurosis measured with three-dimensional ultrasound during isometric contractions. *PeerJ*, 4, e2260.

Raj, I.S., Bird, S.R. & Shield, A.J. (2012) Reliability of ultrasonographic measurement of the architecture of the vastus lateralis and gastrocnemius medialis muscles in older adults. *Clinical Physiology and Functional Imaging*, 32(1), 65–70.

Ravichandiran, K., Ravichandiran, M., Oliver, M.L., Singh, K.S., McKee, N.H. & Agur, A.M.R. (2010) Fibre bundle element method of determining physiological cross-sectional area from three-dimensional computer muscle models created from digitised fibre bundle data. *Computer Methods in Biomechanics and Biomedical Engineering*, 13(6), 741–748.

Schless, S.H., Cenni, F., Bar-On, L., Hanssen, B., Goudriaan, M., Papageorgiou, E. et al. (2019) Combining muscle morphology and neuromotor symptoms to explain abnormal gait at the ankle joint level in cerebral palsy. *Gait and Posture*, 68, 531–537.

Schless, S.H., Cenni, F., Bar-On, L., Hanssen, B., Kalkman, B., O'Brien, T. et al. (2019) Medial gastrocnemius volume and echo-intensity after botulinum neurotoxin A interventions in children with spastic cerebral palsy. *Developmental Medicine and Child Neurology*, 61(7), 783–790.

Schless, S.H., Hanssen, B., Cenni, F., Bar-On, L., Aertbeliën, E., Molenaers, G. et al. (2018) Estimating medial gastrocnemius muscle volume in children with spastic cerebral palsy: a cross-sectional investigation. *Developmental Medicine and Child Neurology*, 60(1), 81–87.

Shortland, A.P., Harris, C.A., Gough, M. & Robinson, R.O. (2002) Architecture of the medial gastrocnemius in children with spastic diplegia. *Developmental Medicine and Child Neurology*, 44(3), 158–163.

Standring, S. (2016) Gray's anatomy 41st edition: the anatomical basis of clinical practice. Gray's anatomy.

Stephensen, D., Drechsler, W. & Scott, O. (2012) Comparison of muscle strength and in-vivo muscle morphology in young children with haemophilia and those of age-matched peers. *Haemophilia*, 18(3), e302–e310.

Tomlinson, D.J., Erskine, R.M., Winwood, K., Morse, C.I. & Onambélé, G.L. (2014) The impact of obesity on skeletal muscle architecture in untrained young vs. old women. *Journal of Anatomy*, 225(6), 675–684.

Vanmechelen, I.M., Shortland, A.P. & Noble, J.J. (2018) Lower limb muscle volume estimation from maximum cross-sectional area and muscle length in cerebral palsy and typically developing individuals. *Clinical Biomechanics*, 51, 40–44.

Weide, G., Huijing, P.A., Maas, J.C., Becher, J.G., Harlaar, J. & Jaspers, R.T. (2015) Medial gastrocnemius muscle growth during adolescence is mediated by increased fascicle diameter rather than by longitudinal fascicle growth. *Journal of Anatomy*, 226(6), 530–541.

Weide, G., Van Der Zwaard, S., Huijing, P.A., Jaspers, R.T. & Harlaar, J. (2017) 3D ultrasound imaging: fast and cost-effective morphometry of musculoskeletal tissue. *Journal of Visualized Experiments*, 55943.

Willerslev-Olsen, M., Choe Lund, M., Lorentzen, J., Barber, L., Kofoed-Hansen, M. & Nielsen, J.B. (2018) Impaired muscle growth precedes development of increased stiffness of the triceps surae musculotendinous unit in children with cerebral palsy. *Developmental Medicine and Child Neurology*, 60(7), 672–679.

Williams, S.A., Stott, N.S., Valentine, J., Elliott, C. & Reid, S.L. (2020) Measuring skeletal muscle morphology and architecture with imaging modalities in children with cerebral palsy: a scoping review. *Developmental Medicine and Child Neurology*, 63(3), 263–273.

Wren, T.A.L., Cheatwood, A.P., Rethlefsen, S.A., Hara, R., Perez, F.J. & Kay, R.M. (2010) Achilles tendon length and medial gastrocnemius architecture in children with cerebral palsy and equinus gait. *Journal of Pediatric Orthopaedics*, 30(5), 479–484.

How to cite this article: Bell, M., Al Masruri, G., Fernandez, J., Williams, S.A., Agur, A.M., Stott, N.S., et al (2021) Typical *m. triceps surae* morphology and architecture measurement from 0 to 18 years: A narrative review. *Journal of Anatomy*, 00, 1–15. https://doi.org/10.1111/joa.13584